Masked fake face detection using radiance measurements

Youngshin Kim, Jaekeun Na, Seongbeak Yoon, and Juneho Yi*

Computer Vision Laboratory, Sungkyunkwan University, 300 Cheoncheon-dong, Jangan-gu, Suwon, Gyeonggi-do 440-746, South Korea
**Corresponding author: jhyi@ece.skku.ac.kr*

Received September 23, 2008; revised December 22, 2008; accepted February 1, 2009; posted February 3, 2009 (Doc. ID 101795); published March 12, 2009

This research presents a novel 2D feature space where real faces and masked fake faces can be effectively discriminated. We exploit the reflectance disparity based on albedo between real faces and fake materials. The feature vector used consists of radiance measurements of the forehead region under 850 and 685 nm illuminations. Facial skin and mask material show linearly separable distributions in the feature space proposed. By simply applying Fisher's linear discriminant, we have achieved 97.78% accuracy in fake face detection. Our method can be easily implemented in commercial face verification systems.

OCIS codes: 100.4998, 240.6645.

1. INTRODUCTION

Reliable fake face detection is essential for a face verification system to be successfully deployed in a real situation such as control of access to secured areas. 2D face printouts or images have usually been used as imposters for unauthorized access. To judge whether the input image contains a real person's face, liveness detection is carried out using motion clues [1] or 3D depth information [2]. However, to our knowledge, studies to detect a fake face that is cleverly disguised with a special makeup mask have not been reported. Considering recent advances in special makeup technology that makes it hard to visually distinguish between masked faces and real faces, the development of masked fake face detection methods is necessary to guarantee a successful face verification system.

This research presents an albedo-3 based method for detecting a masked fake face in a user-cooperative environment, where most practical face verification systems are employed. In a user-cooperative environment, the distance between a person to be verified and the camera, and the person's head pose, are roughly fixed. We exploit the fact that reflectance from real facial skin and mask materials (silicon, latex, or skinjell) should be different. Under the user-cooperative environment of a practical face verification system, we show that computation of albedo can be simplified to the measurement of radiance for a given illumination. This enables us to distinguish between the facial skins and mask materials just by measuring radiance, i.e., gray values in the image.

We have analyzed the distribution of albedo values for illumination of various wavelengths to see how different facial skins and mask materials (silicon, latex, or skinjell) behave in reflectance that is due to material property and surface color. We have found that radiance under 850 nm infrared light is effective for discriminating material property between facial skin and mask materials. In contrast, 685 nm visible light has been reported to be suitable for distinguishing between different facial skin colors of diverse ethnic groups [3]. Thus two radiance measurements under 850 and 685 nm illuminations yield a 2D feature space where facial skin and mask material show linearly separable distributions. For the classification of a feature vector consisting of two radiance measurements under 850 and 685 nm illumination, we applied Fisher's linear discriminant (FLD) [4], which is efficient for discriminating linearly separable distributions, and achieved 97.78% accuracy in fake face detection. In addition, our method is simple enough to be easily implemented in commercial face verification systems.

This paper is organized as follows. Section 2 describes previous work related to the reflectance of materials and albedo. Section 3 shows that measurements of albedo can be simplified to radiance measurements under a user-cooperative environment of a practical face verification system. Based on the findings described in Section 3, Section 4 presents our proposed method to detect masked fake faces, followed by experimental results in Section 5.

2. RELATED WORK

We describe the reflectance of facial skin and silicon. Silicon is popularly used as mask material. We also examine the most recent method for recovering albedo.

A. Reflectance of Slicon and Facial Skin

The ratio of reflected to incident light, albedo, depends not only on the material, thickness, structure, and surface color of the object from which light is reflected but also on the wavelength of the incident light. We investigate the reflectance of real facial skin and silicon material to see whether we can use its difference for discriminating them.

1. Reflectance of Silicon

Silicon, which has been used most widely to make masks, is an elastic solid and is colorless or a little yellow. It is

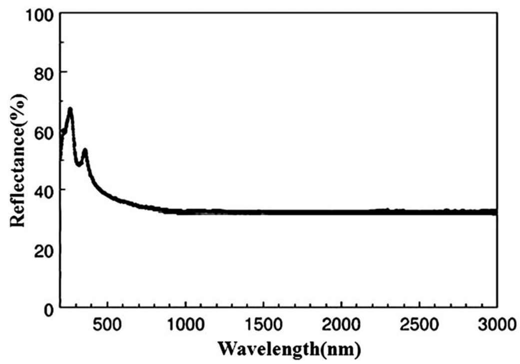

Fig. 1. Reflectance of silicon as the wavelength of light varies [5].

also very flexible and stable over long periods of time. Figure 1 shows the reflectance of silicon surface for the incident light of various wavelength bands. The magnitude of the reflectance of the surface decreases as the wavelength of the light goes from 200 to 900 nm. Beyond 900 nm wavelength, the reflectance remains almost the same, about 30%. Other materials such as latex and skinjell can also be used to make masks. In Section 4, we show that the reflectance of these materials is similar to that of silicon.

2. *Reflectance of Human Skin*

As shown in Fig. 2, human skin is composed of two layers: epidermis and dermis. The external part of the epidermis is made up of subcutaneous fatty tissue [6–9]. Multilayered skin has various light pathways depending on its layers. The stratum corneum directly reflects about 5% of the incident radiation. Larger incident angles result in more reflection. The absorption rate of skin increases and reflection decreases when there is more melanin in the epidermis. The rest of the incident radiation, 95% of the incident light, enters the skin where it is absorbed or scattered within each layer of human skin. The reflectance of human skin depends on scattering and absorption within its various layers [6].

Figure 3 shows the reflectance of human skin of Caucasian and black people. The reflection rate goes up with increasing wavelength. The curves also show that reflectance is influenced by skin color.

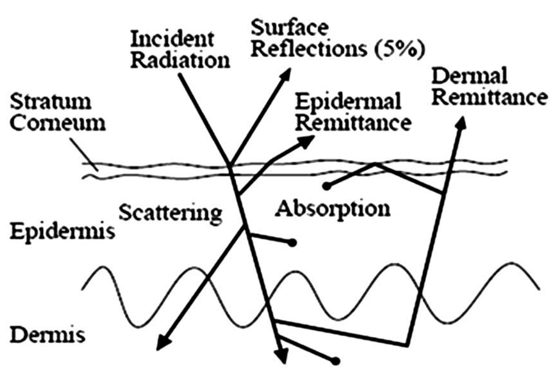

Fig. 2. Schematic representation of light pathways for human skin [6].

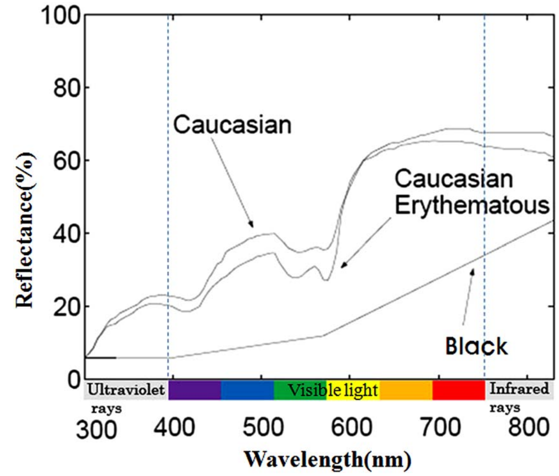

Fig. 3. (Color online) Reflectance of human skin depending on skin color: reflectance from black skin is lower than that of Caucasian skin [6].

3. *Comparison of the Reflectance of Mask Materials and Facial Skin*

In an attempt to find the discriminatory wavelength band of illumination that gives a stable reflectance difference between mask materials and facial skins, we have combined Figs. 1 and 3 to give Fig. 4. We can see the reflectance of silicon, Caucasian skin, and black human skin in Fig. 4. Ultraviolet light in the region of 0–400 nm is harmful to human skin. Infrared equipment that produces light of wavelength greater than 1000 nm is expensive and hard to use. In this research we focus our attention on wavelengths of 850 and 685 nm. We can see that infrared light of 850 nm is discriminatory between facial skins and mask materials in terms of the reflectance disparity. In contrast, 685 nm visible light seems suitable for distinguishing between different facial skin colors. This observation agrees with the results reported in [3].

B. Recovering Albedo

Albedo, defined above as the ratio of reflected to incident radiation, depends on material property and surface color. To recover albedo, photometric stereo methods have gen-

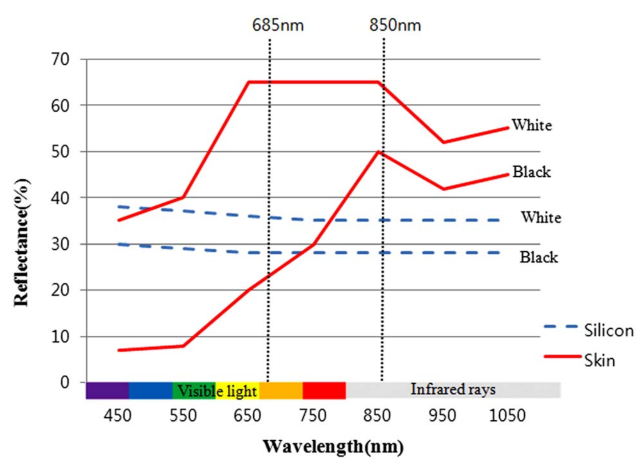

Fig. 4. (Color online) Reflectance of silicon and human skin: the disparity of the reflectance between human skin and mask materials is distinct at 850 nm. Also note that at 685 nm, the reflectance disparity between different skin colors is large.

erally been used, but they require many 2D images [10–13]. Most efficient algorithms represent a collection of 2D images captured as a product of two matrices: one contains albedo and the surface normal information and the other a lighting model. This representation is computed using singular value decomposition (SVD). As shown in Eq. (1), 2D images, M, can be factored into the product of the lighting matrix, $L=U\sqrt{D}$, and the harmonic images, $S=\sqrt{D}V^T$:

$$M=UDV^T=U\sqrt{D}\sqrt{D}V^T \approx L\times S. \tag{1}$$

Each image with unknown lighting conditions is a row in matrix M. The matrix is factored into the product UDV^T by SVD. We can recover the lighting matrix, L, and the harmonic image matrix, S, by reducing ambiguity [14–16]. From the harmonic images, we can obtain shape information about object surfaces that is represented by the surface normal together with albedo estimates. They allow efficient and simple determination of albedo under unknown lighting conditions (position, intensity, etc). However, incorrect albedo may result from inaccurate modeling of lighting. Furthermore, the fact that at least several images need to be captured makes it difficult to apply the method to a practical face verification system.

3. PHOTOMETRIC STEREO METHOD VERSUS RADIANCE METHOD

We show that measurement of albedo can be simplified to radiance measurement when a practical face verification system is deployed under a user-cooperative environment. To detect the albedo of facial skin, we use the forehead region of a face because differences in appearance are smaller there than in other parts of the face. We first extract the forehead region using a simple model-based face detection algorithm [17]. This algorithm detects the forehead region using eye locations and facial geometry. Figure 5 shows typical size and location of the area of a measured forehead. The forehead area is about 220×100 pixels, and the actual size of the forehead region for computing the albedo of facial skin is 100×80 pixels (about 36% of the total forehead area).

In addition, we take only pixels that satisfy Eq. (2) so that we can remove some outliers:

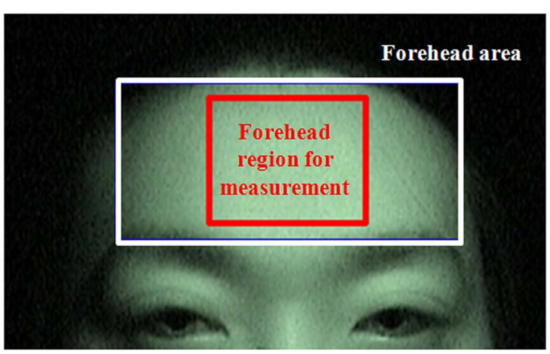

Fig. 5. (Color online) Typical size and location of measured forehead area to detect the albedo of facial skin.

$$|I_i-\mu|\leq k\sigma, \tag{2}$$

where I_i, μ, and σ represent radiance measurement of a pixel in the measurement area, mean value, and standard deviation of I_i, respectively. In actual implementation, $k=1.645$ was used; that is, 10% of the radiance measurements are considered outliers and not used in computing the average value. This makes our method more robust to the presence of scars or spots on the forehead.

Radiance can be represented as in Eq. (3) and is measured as gray value of the image [18]. The gray value at a point in an image can be factorized in an abstract manner to R and G terms. The R factor is concerned with reflectance due to material property and surface color, and the G factor is related to geometry that describes (forehead) shape, illumination, and camera viewpoint. We note that illumination and viewpoint are generally fixed in a user-cooperative environment and that the shape variation of human forehead is very small compared with other parts of the face:

$$I=R\times G. \tag{3}$$

Since the G factor is similar among people, if the surface colors of facial skins and mask materials are approximately the same, the comparison of albedo values between two materials can be simplified to that of their gray values as in Eq. (4). Hence, for a given illumination, we take the average value of the forehead region detected and use it as an estimate of albedo. We call this the radiance method:

$$\frac{I_{face}}{I_{mask}}=\frac{R_{face}\times G_{face}}{R_{mask}\times G_{mask}}\approx\frac{R_{face}}{R_{mask}}. \tag{4}$$

We compare the albedo values from photometric stereo and radiance methods. For photometric stereo, we use the method described in Subsection 2.B. Figure 6 compares the photometric stereo and radiance methods under the environmental condition where the application of Eq. (4) is valid. A yellow-skinned ethnic group was used for Fig. 5, and we applied corresponding makeup to the silicon. The data in this figure are measured by increasing the wavelength of the infrared incident light in 50 nm increments from 750 nm to 1000 nm. The reflectance disparity between facial skin and silicon becomes more evident in the case of the radiance method than with the photometric stereo method. We have conducted the experiments under the environment with and without ambient light and have obtained similar results. We can see that the radiance method is the more efficient method for discriminating between facial skin and silicon material. Furthermore, the radiance method exploits only a single 2D image.

4. MASKED FAKE FACE DETECTION USING THE RADIANCE METHOD

In this section, we analyze the distribution of albedo values between facial skin and the mask materials (silicon, latex, and skinjell) using the radiance method as we vary the wavelength of illumination. Different skin colors are

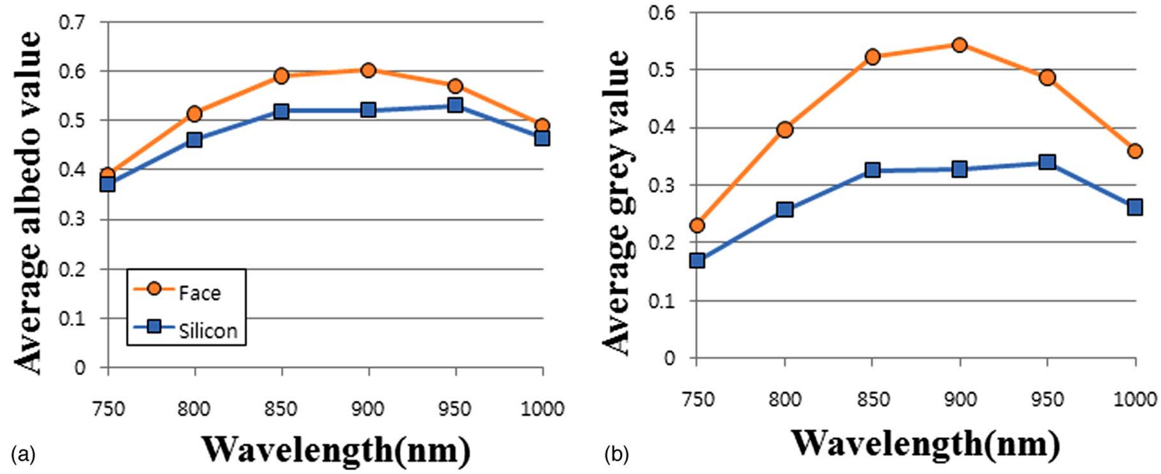

Fig. 6. (Color online) Reflectance with the photometric stereo method and the radiance method: (a) Average albedo value using four images for the photometric stereo method, (b) average gray value from a single image for the radiance method. The reflectance disparity between human skin and silicon material is greater when the radiance method is used.

considered in Subsection 4.B. In Subsection 4.C we describe the effect of wearing oil-based or regular makeup.

A. Albedo for Light of Different Wavelengths

To find the discriminatory wavelength band of light that gives a stable reflectance disparity between mask materials and facial skin, we experimented with four monochromatic visible lights and three infrared lights at wavelengths of 750, 850, and 970 nm.

1. Monochromatic Visible Light

We have illuminated monochromatic visible light on mask materials and human skin and compared their reflectance. Four colors are considered: red, green, blue, and yellow. As can be seen in Fig. 7, none of these monochromatic visible lights provides a stable reflectance disparity between mask materials and facial skin.

2. Infrared Light

When we use infrared light, the reflection is less affected by surface color. Illumination using light of wavelength beyond 1000 nm is very costly and is not considered in this research because we aim at applicability in a practical system. We focus on 750, 850, and 970 nm wavelengths of light. Figure 8 shows the reflectance of facial skin and mask materials (i.e., silicone, latex, and skinjell) in these three wavelength bands of light.

In this experiment, we have used an infrared filter to eliminate the influence of visible light. We obtain low reflectance values at 750 nm because the filter also screens out infrared light near the visible light range. 970 nm light does not give a clear separation in reflectance between the facial skins and mask materials. Their reflectance is influenced by noise and error. In contrast, we can see a stably separable reflectance disparity between facial

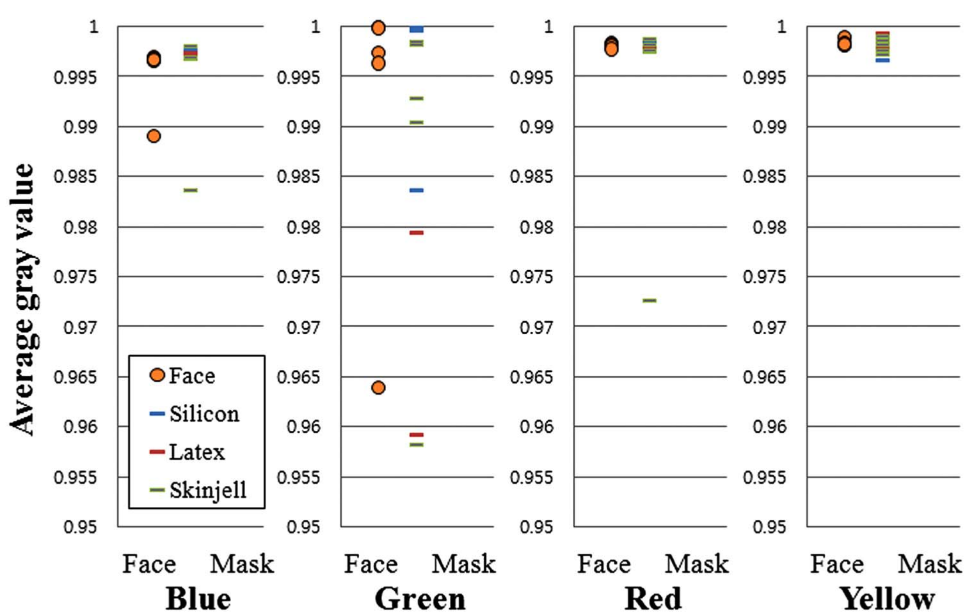

Fig. 7. (Color online) Reflectance of facial skin and mask materials for four different colors of visible light.

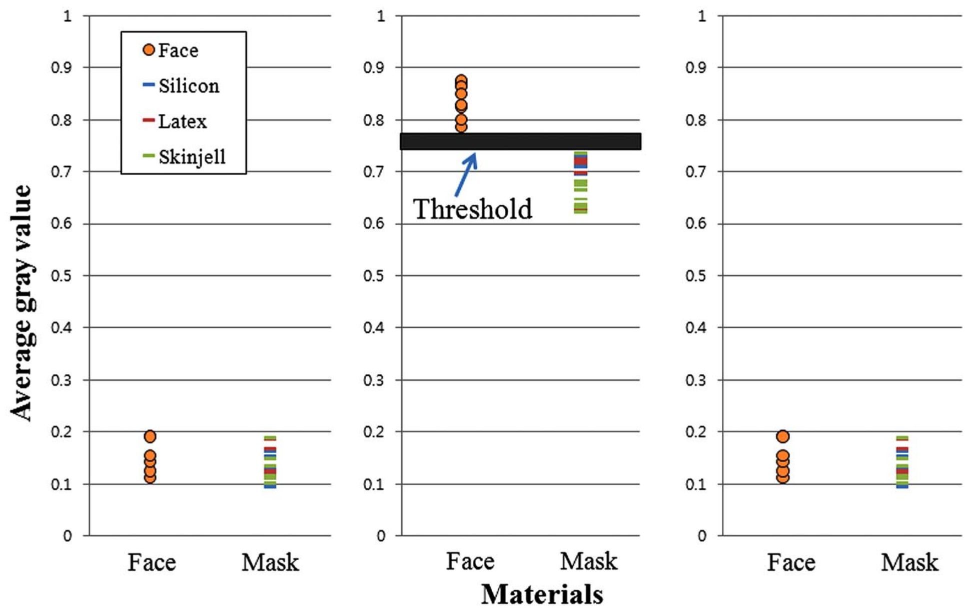

Fig. 8. (Color online) Reflectance of human skin and mask materials for infrared light with wavelengths of 750, 850, and 970 nm: At 850 nm, reflectance between human skin and mask materials is stably separable.

skins and mask material at 850 nm. Hence, we use 850 nm infrared light to distinguish between facial skins and mask materials.

B. Feature Vector Proposed

We also consider colors of facial skin and mask materials. Although both water-based and oil-based paints can be used for mask painting, oil-based paint is generally preferred for painting masks because water-based paint can be easily rubbed off. Thus, we investigate variations in reflectance with respect to mask materials painted with oil-based paint. We have painted the mask surface to make it look like the facial skin colors of black-, yellow-, and white-skinned ethnic groups with the aid of a professional special makeup artist. We then measure the difference in reflectance between real facial skins of different races and the painted mask materials.

As mentioned in Subsection 2.A, we exploit the reflectance at 685 nm to distinguish skin colors because this wavelength is the most sensitive to color variations in visible light. On the other hand, we have found in Subsection 4.A that infrared light of 850 nm is effective for discriminating material property between facial skin and mask material using reflectance disparity. We create a 2D feature vector of which two elements are the radiance values under 850 and 685 nm illumination. Figure 9 shows a linearly separable distribution of feature vectors for real facial skins and mask materials. We can see that the fea-

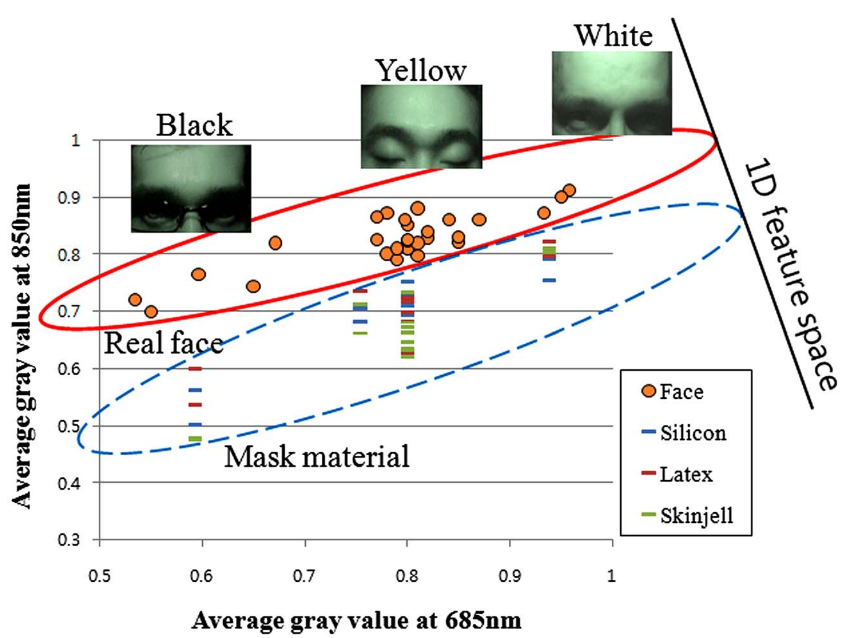

Fig. 9. (Color online) Feature space proposed.

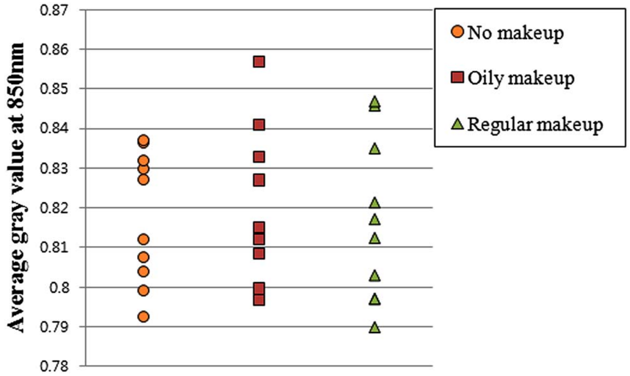

Fig. 10. (Color online) Variation of albedo for oily and regular makeup.

ture vector proposed has discriminatory power for detecting masked fake faces.

C. Effect of Makeup

For a clear description of experimental results we have conducted the experiments on faces with oily or regular makeup to see how cosmetics affect the results. We used oily lotion for oily makeup, and regular lotion, makeup base, foundation, and powder for regular make-up. As can be seen in Fig. 10, there is little variation in reflectance due to makeup. We think this is because the diffuse component of reflection comes from the light that has penetrated some distance (enough to pass the makeup layer) into the surface, to be refracted and reflected until it re-emerges from the surface layer.

Too oily skin can violate the assumption of Lambertian surface in the general condition. However, in our case, its effect can be tolerable. Oily skin surfaces have both diffuse and glossy reflections, and diffuse reflection plays a major role in our research. The strong max radiance, i.e., highlight due to glossy reflection, is visible only where the surface normal is oriented halfway between the direction of the incoming light and the direction of the viewer. As can be seen in Fig. 11 of our setup, the camera cannot see the highlight. The weak max radiance due to diffuse reflection can occur because the surface normal and the viewing direction of the camera are parallel. In the forehead region used for our method, the variation of the surface normal is not significant enough to observe highlight from any specific location.

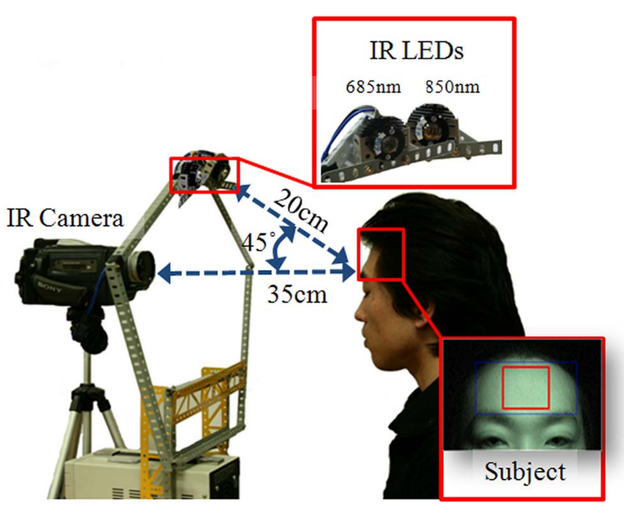

Fig. 11. (Color online) Sketch of the experimental setup.

5. EXPERIMENTAL RESULTS

Figure 11 shows the experimental setup. The distances from the center of forehead region to the two LED light sources [19] of 685 and 850 nm wavelengths and the camera are 20 and 35 cm, respectively. The angle between each LED light source and the camera is 45°. We turn on the two LED lights consecutively and take the average gray values of the forehead skin using the pixel values that satisfy Eq. (2).

Since it is difficult for us to obtain ample data with respect to various skin colors, we have not only used our experimental data (white-skinned subjects, 15; yellow-skinned subjects, 175; and black-skinned subjects, 15) but also refer to previous research data [3]. The data are divided into two groups. The first group of 112 visible and infrared images is used for training, and the second group of 93 images for testing.

We obtain a 2D feature vector that consists of two average radiance measurements from 685 and 850 nm illuminations. For the classification of the feature vector, we have employed Fisher's linear discriminant (FLD). FLD is a very efficient classifier that can distinguish data distributed in a linearly separable fashion. A feature vector is projected onto a subspace of dimensionality $C-1$. C denotes the number of classes (i.e., $C=2$ in our case, real face or masked face). The resulting 1D subspace is also shown in Fig. 9. Table 1 shows the experimental results. We have achieved 97.78% accuracy in fake face detection. The cause of error is threefold. First, although we assume a user-cooperative environment, sometimes we observe that the variation of the participant's head pose is greater than allowed. When the head is tilted up, we typically see some weak highlight region from the forehead area whose surface normal lies in the direction of the camera's viewing direction. When the head is tilted down, the image intensity is relatively low. This yields a wrong average radiance value. Second, the performance of our method also depends on that of the algorithm used to detect the forehead region. We have excluded the cases of incorrect detection of forehead region. Third, as can be seen in Fig. 9, separability between Caucasian skin type and mask material is relatively low compared with other skin types.

For now, we reserve our claim on Caucasian skin type because of the lack of Caucasian skin data. Geographically, it is too difficult to collect a large number of Caucasian skin data at our location. When we are able to collect

Table 1. Results of Masked Fake Face Detection Using Radiance Measurements

Type of Image	Detection Rate	
	Correct	Wrong
Real face	95.74%	4.26%
Mask	97.78%	2.22%
Total	96.77%	3.23%

more Caucasian skin data, we would like to extend our research so that it can include Caucasian skin type. We think it is reasonable to include black skin type even though there are fewer data than for yellow skin type, because black skin type shows a significant difference in reflectance from mask material (refer to Fig. 9).

6. CONCLUSIONS AND DISCUSSION

In this paper, we have proposed a method for masked fake face detection that uses reflectance disparity, namely albedo. We have presented a feature vector that effectively discriminates between masked fake faces and real faces. First, considering a practical face verification system that is deployed under a user-cooperative environment, we have shown that computation of albedo can be simplified just to measurements of gray values in the image captured. We have found that infrared light at 850 nm is discriminatory enough to distinguish between facial skins and mask materials using reflectance disparity. On the other hand, visible light at the wavelength of 685 nm has been reported to be suitable for distinguishing the different facial skin colors of different ethnic groups. We have shown that the 2D feature vector that consists of radiance measurements under 850 and 685 nm illuminations has the discriminatory power to distinguish between real faces and masked fake faces. We have employed FLD to successfully discriminate between facial skins and mask materials whose distributions are linearly separable in the proposed 2D feature space. Our method is capable of detecting masked fake faces in real time and can be readily implemented in commercial face verification systems.

REFERENCES

1. F. Bettinger and T. F. Cootes, “A model of facial behaviour,” in *Proceedings of IEEE Conference on Automatic Face and Gesture Recognition* (IEEE, 2004), pp. 123–128.
2. J. Park, C. Kim, J. Na, and J. Yi, “Effectively exploiting distortion of structured light pattern for capturing depth discontinuities,” in *Proceedings of the 13th Japan–Korea Joint Workshop on Frontiers of Computer Vision* (2007), pp. 29–34.
3. N. G. Jablonski and G. Chaplin, “The evolution of human skin coloration,” J. Human Evolution **39**, 57–106 (2000).
4. R. O. Duda, P. E. Hart, and D. G. Stork, *Pattern Classification*, 2nd ed. (Wiley-Interscience, 2000).
5. K. Hadobás, S. Kirsch, A. Carl, M. Acet, and E. F. Wassermann, “Reflection properties of nanostructure-arrayed silicon surfaces,” Nanotechnology **11**, 161–164 (2000).
6. M. Störring, “Computer vision and human skin colour,” in Ph.D. dissertation (Computer Vision and Media Technology Laboratory, Aalborg University, Denmark, 2004).
7. E. Angelopoulou, “The reflectance spectrum of human skin,” Tech. Rep. MS-CIS-99-29 (Pennsylvania University, 1999).
8. C. Donner and H. W. Jensen, “A spectral BSSRDF for human skin,” in *Proceedings of Eurographics Symposium on Rendering Techniques* (2006), pp. 409–417.
9. C. Donner and H. W. Jensen, “Light diffusion in multilayered translucent material,” in *Proceedings of ACM SIGGRAPH 2005 Papers* (ACM SIGGRAPH, 2005) pp. 1032–1039 (siggraph. org).
10. R. Basri and D. Jacobs, “Photometric stereo with general, unknown lighting,” in *Proceedings of IEEE Conference on Computer Vision and Pattern Recognition* (IEEE, 2001), pp. 374–381.
11. H. Hayakawa, “Photometric stereo under a light source with arbitrary motion,” J. Opt. Soc. Am. A **11**, 3079–3089 (1994).
12. A. L. Yuille, D. Snow, R. Epstein, and P. N. Belhumeur, “Determining generative models of objects under varying illumination: shape and albedo from multiple images using SVD and integrability,” Int. J. Comput. Vis. **35**, 203–222 (1999).
13. I. Kemelmacher and R. Basri, “Indexing with unknown illumination and pose,” in *Proceedings of IEEE Conference on Computer Vision and Pattern Recognition* (IEEE, 2005), pp. 909–916.
14. P. N. Belhumeur, D. J. Kriegman, and A. L. Yuille, “The bas-relief ambiguity,” in *Proceedings of IEEE Conference on Computer Vision and Pattern Recognition* (IEEE, 1997), pp. 1060–1066.
15. R. Epstein, A. L. Yuille, and P. N. Belhumeur, “Learning object representations from lighting variations,” in *Proceedings of European Conference on Computer Vision* (Springer-Verlag, 1996), pp. 179–199.
16. A. Yuille and D. Snow, “Shape and albedo from multiple images using integrability,” in *Proceedings of IEEE Conference on Computer Vision and Pattern Recognition* (IEEE, 1997), pp. 158.
17. W. Huang and R. Mariani, “Face detection and precise eyes location,” in *Proceedings of IEEE Conference on Computer Vision and Pattern Recognition* (IEEE, 2000), Vol. 4, pp. 722–727.
18. S. G. Narasimhan, V. Ramesh, and S. K. Nayar, “A class of photometric invariants: separating material from shape and illumination,” in *Proceedings of IEEE International Conference on Computer Vision* (IEEE, 2003), Vol. 2, pp. 1387–1394.
19. Roithner LaserTechnik Co., http://www.roithner-laser.com.